運輸省港湾技術研究所

港湾技術研究所報告

REPORT OF THE PORT AND HARBOUR RESEARCH INSTITUTE

MINISTRY OF TRANSPORT

VOL. 24 NO. 3 SEPT. 1985

NAGASE, YOKOSUKA, JAPAN

港湾技術研究所報告 (REPORT OF P.H.R.I.)

第24巻　第3号 (Vol. 24, No. 3), 1985年9月 (Sept. 1985)

目　　次 (CONTENTS)

REPORT OF THE PORT AND
HARBOUR RESEARCH INSTITUTE
Vol. 24, No. 3 (Sept. 1985)

1. Characteristics of Ocean Waves off Cape Nojima in the Northwestern Pacific, Measured with a Discus Buoy

Koji KOBUNE*
Hiroshi SASAKI**
Noriaki HASHIMOTO***

Synopsis

The sea area to the southeast of Cape Nojima has been called as the dangerous sea. A number of large ships have been involved in sea disasters there.

As a part of a comprehensive study conducted by the Ministry of Transport to promote maritime safety, a discus buoy had been set up at the location 147°E in longitude and 32°N in latitude, and ocean waves as well as weather condition in the sea area had been measured from October 1983 to June 1984.

The wave data were analyzed at the Port and Harbour Research Institute. The results of statistical analysis show that the significant wave heights during the winter were about twice to threefold as large as these observed in the Pacific coastal sea area, and that the ratios between the characteristic wave parameters such as H_{max}/H_s, and the cumulative distribution of relative significant wave heights ($H_s/\overline{H}_s$) are similar to those obtained from coastal wave deta. The time variation of the significant wave height and the mean wave direction were closely related with the variation of the wind speed and the wind direction on the spot respectively, espcially for large waves ($H_s \geqq 4$m) which were seen when the wind speed exceeded 15 m/s.

In addition, the mode of the directional spectra is examined on the basis of the relation between the directional parameters, i. e. the long-crestedness and the mean spreading angle. The directional spectrum for extreme seas off Cape Nojima is supposed to be either unimodal one characterized by the Mitsuyasu type directional functions with $s_{max}=10$ to 40 or bimodal one having two directional peaks of which difference in direction is less than 90°.

* Chief of Coastal Observation Laboratory, Hydraulic Engineering Division
** Senior Research Engineer, Hydraulic Engineerig Division
*** Member of Storm Surge and Tsunami Laboratory, Hydraulic Engineering Division

港湾技術研究所報告
第24巻 第3号 (1985. 9)

1. ディスカス・ブイで観測された野島崎沖海域の波浪特性

小舟浩治*・佐々木弘**・橋本典明***

要旨

野島崎沖海域においては，これまで大型船を含む多数の船が海難に遭遇しており，沿岸部の波浪からは予想もつかないような特異な波浪が発生しているのではないかと懸念されていた。

本研究は，このように頻発する海難の防止を目的として運輸省が進めている総合的研究の一環として実施されたものであり，1983年10月から翌年6月まで実施されたブイによる波浪観測記録を解析し，これまでに知られている沿岸部の波浪の特性と比較検討を行ったものである。

当海域における冬期の波浪は，一般に沿岸部の2～3倍の有義波高となっている。しかし，波群の特性値（H_{max}/H_s，$H_s/\overline{H}$ など），有義波高（$H_s/\overline{H}_s$）の発生確率，有義波高と周期の結合確率分布形状等は，沿岸部におけるものと類似していることが知られた。また，有義波高及び平均波向は，それぞれ風速，風向の経時変化に追随して変動しており，特に海難が発生するような波高の大きい場合には，この海域上の風の場により発生する風波が支配的であり，他の波源から到達するうねりの寄与は小さいものと考えられる。

さらに，波浪の方向分布に関する二種類のパラメータ（峯波長パラメータ及び平均分散角）が，方向スペクトル形状に応じた一定の関係にあることを示し，この特性を利用して，波浪の方向スペクトルが単峯型であるか双峯型であるかを判別しうることを確かめた。この方法により観測波浪のスペクトル形状を検討した結果，有義波高が6mを越えるような高波については，その方向スペクトルは単峯型に近い形（光易型方向関数において s_{max}=10程度）か，あるいは双峯型と仮定しても，二つの方向差は90°以下であるような形状と推定された。

* 水工部 海象観測研究室長
** 水工部 主任研究官（海象測定技術担当）
*** 水工部 高潮津波研究室

CONTENTS

1. Introduction

The sea area which lies to the southeast of the Japan Islands provides one of the busiest ocean routes in the world. A lot of large ships are plying between Japan and North and Sonth America. However, the weather over the sea area is very changeable in winter. Atmospheric depressions are generated one after another in the western area and move fast towards the east as they grow until they disappear in the North Pacific Ocean. This kind of meteorological disturbance causes severe rough seas in this area. As a matter of fact, a number of vessels have been involved in sea disasters. Some of them are the Boriver-maru (lost on Jan. 5, 1969), the California-maru (lost on Feb. 9, 1970), and the Onomichi-maru (damaged on Dec. 28, 1980). Since 1969, at least 14 large vessels which had the tonnages more than 10,000 have met shipwreck. All the accidents happened in the period from October to February. Figure 1 shows the location where these sea disasters occurred. The sea area to the east-southeast of Cape Nojima, thus, has been called as the dangerous sea area.

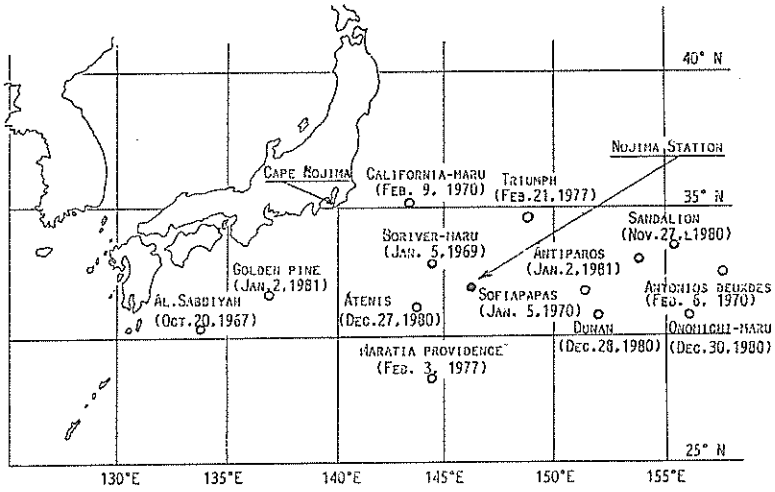

Fig. 1 Locations where Sea Disaster Occurred

The barometric pressure system over the Japan Islands and the east part of Asian Continent generates so-called monsoons. During the winter, a typical pattern of the system is such that a high pressure is located to the west and a low pressure exists to the east of the Japan Islands; the pressure pattern brings a predominant northwestern monsoon.

This typical pressure system is often disturbed by a local atmospheric depression which appears in the sea area under discussion. This kind of a complex pressure system has been suspected to generate a complex sea state which might be called as bi-directional seas where two wave groups generated by the monsoon and the local depression interact to each other. The complex sea state can yield incredibly huge waves of unusual nature such as pyramidal waves or freak waves, which might have caused the above-mentioned sea disasters.

From the viewpoint of improving maritime safety, the Ministry of Transport in cooperation with its attached agencies, i.e., the Japan Meteorological Agency, the Meteorological Research Institute, the Ship Research Institute, and the Port and Harbour Reseach

Institute, has been conducting a comprehensive study on the sea disasters in the area concerned. The study consists of wave observation at the sea area, analysis of the wave action on the hull of vessels, prototype measurement of ship motions and wave pressure utilizing a patrol boat of the Maritime Safety Agency, hydraulic model tests of the interaction between waves and wind and that between ocean current and wind generated waves and numerical simulations for wave forecasting.

A discus buoy was employed for the wave observation, and it had been placed in the sea area from October 1983 to June 1984. The buoy made the measurement of waves and several quantities related to weather conditions every three hours and it transmitted the data via the geo-stationary weather satellite "Himawari (Sunflower)" to the Meteorological Agency. Having been edited by the Agency, the wave and weather data were disrtibuted to the agencies involved in the study. The statistical characteristics of waves and some aspects of extreme sea states have been studied at the Port and Harbour Research Institute with an emphasis on the characteristics of directional wave spectra. In addition, some characteristic parameters associated with directional wave spectra are compared with those obtained from the wave data at several coastal observation stations.

2. Literature Survey on Directional Wave Measurements

2.1 Estimation of Directional Wave Spectra

Several methods and principles have been developed for the estimation of directional wave spectra. So far, many measurements of the directional wave have been utilizing pitch and roll buoys and two-axis current meters. Longuet-Higgins et. al.[1] developed a directional buoy which measures the heave acceleration and the angles of pitch and roll, and they proposed a principle of the estimation of directional spectra from the time series records of these three quantities. The principle is summarized as follows.

With the assumption that the profiles of random ocean waves can be expressed as a linear superposition of sinusoidal component waves, three quantities measred by a pitch and roll buoy are expressed as

$$\left.\begin{aligned}
&\eta=\sum_{n=1}^{\infty}a_n\cos\left(k_nx\cos\theta_n+k_ny\sin\theta_n-\omega_nt+\varepsilon_n\right),\\
&\eta_x=\frac{\partial\eta}{\partial x}=-\sum_{n=1}^{\infty}k_na_n\cos\theta_n\sin\left(k_nx\cos\theta_n+k_ny\sin\theta_n-\omega_nt+\varepsilon_n\right),\\
&\eta_y=\frac{\partial\eta}{\partial y}=-\sum_{n=1}^{\infty}k_na_n\sin\theta_n\sin\left(k_nx\cos\theta_n+k_ny\sin\theta_n-\omega_nt+\varepsilon_n\right).
\end{aligned}\right\}\qquad(1)$$

where η, η_x and η_y are heave, pitch and roll respectively, and the heave is obtained from the double integration of heave acceleration with respect to time.

The autocorrelation functions and the covariance functions between these three quantities are calculated by the following equations :

$$\left.\begin{aligned}
&\Psi_{11}(\tau)=\overline{\eta(t)\eta(t+\tau)}=\sum_{n=1}^{\infty}\frac{1}{2}a_n^2\cos\omega_n\tau,\\
&\Psi_{22}(\tau)=\overline{\eta_x(t)\eta_x(t+\tau)}=\sum_{n=1}^{\infty}\frac{1}{2}k_n^2a_n^2\cos^2\theta_n\cos\omega_n\tau,\\
&\Psi_{33}(\tau)=\overline{\eta_y(t)\eta_y(t+\tau)}=\sum_{n=1}^{\infty}\frac{1}{2}k_n^2a_n^2\sin^2\theta_n\cos\omega_n\tau,
\end{aligned}\right\}\qquad(2)$$

$$\left.\begin{aligned}
\Psi_{12}(\tau)&=\overline{\eta(t)\eta_x(t+\tau)}=\sum_{n=1}^{\infty}\frac{1}{2}k_n a_n^2\cos\theta_n\sin\omega_n\tau,\\
\Psi_{13}(\tau)&=\overline{\eta(t)\eta_y(t+\tau)}=\sum_{n=1}^{\infty}\frac{1}{2}k_n a_n^2\sin\theta_n\sin\omega_n\tau,\\
\Psi_{23}(\tau)&=\overline{\eta_x(t)\eta_y(t+\tau)}=\sum_{n=1}^{\infty}\frac{1}{2}k_n^2 a_n^2\cos\theta_n\sin\theta_n\cos\omega_n\tau.
\end{aligned}\right\}$$

From these autocorrelation functions and the covariance functions, cross-spectra are calculated by Eq. (3).

$$\left.\begin{aligned}
C_{11}(f)&=\int_{-\infty}^{\infty}\Psi_{11}(\tau)\cos 2\pi f\tau\,d\tau=\frac{1}{2}\int_0^{2\pi}S(f,\ \theta)d\theta,\\
C_{22}(f)&=\int_{-\infty}^{\infty}\Psi_{22}(\tau)\cos 2\pi f\tau\,d\tau=\frac{1}{2}\int_0^{2\pi}S(f,\ \theta)k^2\cos^2\theta\,d\theta,\\
C_{33}(f)&=\int_{-\infty}^{\infty}\Psi_{33}(\tau)\cos 2\pi f\tau\,d\tau=\frac{1}{2}\int_0^{2\pi}S(f,\ \theta)k^2\sin^2\theta\,d\theta,\\
Q_{11}(f)&=Q_{22}(f)=Q_{33}(f)=0,\\
C_{23}(f)&=\int_{-\infty}^{\infty}\Psi_{23}(\tau)\cos 2\pi f\tau\,d\tau=\frac{1}{2}\int_0^{2\pi}S(f,\ \theta)k^2\cos\theta\sin\theta\,d\theta,\\
Q_{12}(f)&=\int_{-\infty}^{\infty}\Psi_{12}(\tau)\sin 2\pi f\tau\,dt=\frac{1}{2}\int_0^{2\pi}S(f,\ \theta)k\cos\theta\,d\theta,\\
Q_{13}(f)&=\int_{-\infty}^{\infty}\Psi_{13}(\tau)\sin 2\pi f\tau\,d\tau=\frac{1}{2}\int_0^{2\pi}S(f,\ \theta)k\sin\theta\,d\theta,\\
C_{12}(f)&=C_{13}(f)=Q_{23}(f)=0.
\end{aligned}\right\}\qquad(3)$$

Thus the relation between the integrals of the directional spectrum $S(f,\ \theta)$ and the cross-spectra and the autocorrelation functions of six quantities are obtained.

Let the directional spectrum $S(f,\ \theta)$ be expressed in a Fourier series as follows:

$$S(f,\ \theta)=\frac{1}{2}A_0(f)+\sum_{n=1}^{\infty}[A_n(f)\cos n\theta+B_n(f)\sin n\theta].\qquad(4)$$

By substituting the above equations for the $S(f,\ \theta)$ into Eq. (3), and by carrying out the integrations, the Fourier coefficients for $n=0$, 1, and 2 can be determined as

$$\left.\begin{aligned}
A_0(f)&=\frac{2}{\pi}C_{11}(f),\quad A_1(f)=\frac{2}{\pi k}Q_{12}(f),\quad A_2(f)=\frac{2}{\pi k^2}[C_{22}(f)-C_{33}(f)],\\
B_1(f)&=\frac{2}{\pi k}Q_{13}(f),\quad B_2(f)=\frac{4}{\pi k^2}C_{23}(f).
\end{aligned}\right\}\qquad(5)$$

The resultant estimate of the directional spectrum consists of only up to the second-order terms of the infinite Fourier series. Therefore, it is a biased estimate of the true spectrum. In order to get better estimates, Longuet-Higgins et. al. proposed the use of the following formula for the estimation of the directional spectra.

$$\hat{S}(f,\ \theta)=\frac{1}{2}A_0+\frac{2}{3}(A_1\cos\theta+B_1\sin\theta)+\frac{1}{6}(A_2\cos 2\theta+B_2\sin 2\theta).\qquad(6)$$

Mitsuyasu et. al.[2] developed a cloverleaf buoy which measures the curvature of the water surface in addition to the pitch, roll and heave of the buoy, and proposed a standard form of the direcdional spreading function of ocean waves on the basis of their measurement of directional spectra. The proposed directional spreading function is as follows:

$$G(f,\ \theta)=G_0\cos^{2s}(\theta/2),\qquad(7)$$

where G_0 is the proportionality constant, θ is the direction measured counterclockwise from the mean wave direction, and s is the spreading parameter. The value of this parameter varies with the frequency as given by Eq. (8); it takes the maximum value s_{max} for the peak frequency of the power spectrum and decrease as the frequency deviates from the peak frequency.

$$s=\begin{cases} s_{max}(f/f_p)^5 & : f\leq f_p \\ s_{max}(f/f_p)^{-2.5} & : f\geq f_p \end{cases} \tag{8}$$

If it is assumed that the directional spectrum is spread over the range from $\theta_{min}=-\pi$ to $\theta_{max}=\pi$, G_0 is given by Eq. (9).

$$G_0=\frac{1}{\pi}2^{2s-1}\frac{\{\Gamma(s+1)\}^2}{\Gamma(2s+1)} \tag{9}$$

where Γ ( ) denotes the Gamma function.

For a wave gauge array, Capon et. al.[3] developed the maximum likelihood method to obtain a better estimate of directional spectrum. Isobe et. al.[4] extended that method so that the method can be applied for a combination of arbitrary quantities, i.e., water surface elevation, water particle velocities, surface slopes, pressure, etc. Isobe et. al. named it the extended maximum likelihood method. In this method, the directional spectrum is calculated by Eq. (10).

$$\hat{S}(k,\ \omega)=\kappa/[\sum_m\sum_n \Phi_{mn}^{-1}(\omega)H_m^*(k,\ \omega)H_n(k,\ \omega)e^{ik(x_n-x_m)}] \tag{10}$$

where $H_n(k,\ \omega)$ is the transfer function from water surface elevation to other wave property η_n, the superscript $*$ denotes the conjugate complex, Φ_{mn}^{-1} denotes the $(m,\ n)$ component of the inverse matrix of the complex matrix of the conjugate cross-spectrum $\Phi_{ij}=C_{ij}+iQ_{ij}$, and κ is the proportionality constant which is determined to satisfy the following relation.

$$\Phi_{11}(\omega)=\int_k \hat{S}(k,\ \omega)dk \tag{11}$$

2.2 Wave Direction and Parameters Associated with Directional Spectrum

The wave direction is a quantity which eludes quantative definition. No standard method has been developed for the determination of wave direction as a group. Even though a wave directional spectrum is estimated from the measurement utilizing a pitch and roll buoy or a pair of directional current meters, the predominant direction varies from frequency to frequency. A possible definition of the wave direction is the predominant wave direction at the peak frequency at which the power spectrum shows the maximum. Another alternative is to define wave directions for frequency by frequency. However, from a viewpoint of the consistency with the conventional directional measurements, i.e., the optical technique such as the use of imaging radar and stereophotogrametry, it is desired to define a single wave direction for a whole wave group.

(1) Mean and principal wave directions

For a random wave gruop having a directional spectrum denoted by $E(l,\ m)$ in the Cartesian coordinates of wave number domain $(l,\ m)$ where $l=k\cos\theta$, $m=k\sin\theta$, Longuet-Higgins[5] gave the definition of the mean and the principal wave direction, i.e. $\bar{\theta}$ and θ_p, as follows:

$$\bar{\theta}=\tan^{-1}(\bar{m}/\bar{l})=\tan^{-1}(M_{01}/M_{10}), \tag{12}$$

$$\theta_p=\frac{1}{2}\tan^{-1}\left(\frac{2M_{11}}{M_{20}-M_{02}}\right), \tag{13}$$

where

$$\left.\begin{aligned} &\bar{m}=M_{01}/M_{00}, \qquad \bar{l}=M_{10}/M_{00}, \\ &M_{pq}=\int_{-\infty}^{\infty}\int_{-\infty}^{\infty}E(l,\ m)l^p m^q\,dl\,dm, \end{aligned}\right\} \tag{14}$$

As the quantities $\bar{l}$ and $\bar{m}$ in Eq. (12) represent the abscissa and the ordinate of the center of gravity of the directional spectrum respectively, $\bar{\theta}$ denotes the directon of the center of gravity drawn from the origin of the coordinates, as shown in Fig. 2. On the other hand, the principal wave direction θ_p denotes the direction along which the root-mean-square wave number is largest, or the wave crests are the densest. By definition, θ_p is given in the range from $-\pi/2$ to $\pi/2$, while $\bar{\theta}$ is given in full range ($-\pi$ to π).

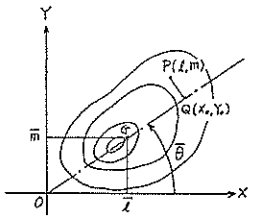

Fig. 2 Sketch of Directional Spectrum

(2) Parameters associated with directional spectrum

Longust-Higgins[5] further proposed the parameter named the long-crestedness, which is an index of the directional spreading of random sea. The parameter is defined by Eq. (15)

$$\gamma=\left\{\frac{(M_{20}+M_{02})-\sqrt{(M_{20}-M_{02})^2+4M_{11}^2}}{(M_{20}+M_{02})+\sqrt{(M_{20}-M_{02})^2+4M_{11}^2}}\right\}^{1/2} \tag{15}$$

The parameter γ is the ratio of the root-mean-square of the variance of the wave directional spectrum about the principal direction (minimum value) and that about the direction perpendicular to the formar (maximum value). The parameter γ takes the value zero for unidirectional waves and takes 1.0 for directional homogeneity.

Goda[6),7)] examined in detail the two definitions of wave direction and the long-crestedness, especially for bimodal directional wave systems, which is formed when swell and wind generated waves of similar magnitudes are coming from the directions quite different from each other. He illustrated the behavior of the principal direction θ_p and the long-crestedness for the case of bi-directional wave system. On the basis of the examination, Goda recommended the use of the mean wave direction rather than the principal wave direction, and commented that the long-crestedness is not an appropriate parameter as the index of the bimodality of directional spectra. He further proposed an alternative parameter named the mean spreading angle θ_k. It is defined by Eq. (16)

$$\theta_k=\tan^{-1}(R/\bar{k})=\tan^{-1}\left\{\frac{\sqrt{M_{00}}\sqrt{M_{01}^2M_{20}-2M_{10}M_{01}M_{11}+M_{10}^2M_{02}}}{M_{10}^2+M_{01}^2}\right\}, \tag{16}$$

where $\bar{k}$ denotes the mean wave number ($\overline{k^2}=\overline{l^2}+\overline{m^2}$), and R is the root-mean-square wave number of the directional spectrum about the mean direction. The root-mean-square wave number R is calculated by Eq. (17).

$$R^2=\frac{1}{M_{00}}\int_{-\infty}^{\infty}\int_{-\infty}^{\infty}E(l,m)\overline{PQ}^2\,dl\,dm=\frac{M_{01}^2M_{20}-2M_{10}M_{01}M_{11}+M_{10}^2M_{02}}{M_{00}(M_{10}^2+M_{01}^2)}, \tag{17}$$

where $\overline{PQ}$ is the distance between the point $P(l,\ m)$ and the axis which passes through

the origin O and the center of gravity of the directionary spectrum G (see Fig. 2).

The mean spreading angle θ_k takes the value zero for unidirectional waves and 90 degress for the waves with directional homogeneity.

Goda also proposed a practical method to calculate the wave directions $\bar{\theta}$ and θ_p and the two parameters γ and θ_k from the covariances between the quantities related to wave motions. The proposed method does not require the computation of directional wave spectrum and makes it possible to calculate the wave direction and the parameters by on-board real time analysis with microprocessors. For the case of directional wave measurement with a pitch and roll buoy, the wave directions $\bar{\theta}$ and θ_p and the parameters γ and θ_k are calculated by the following equations:

$$\bar{\theta}=\tan^{-1}(\overline{\eta_t\eta_y}/\overline{\eta_t\eta_x}), \tag{18}$$

$$\theta_p=\frac{1}{2}\tan^{-1}[2\overline{\eta_x\eta_y}/(\overline{\eta_x^2}-\overline{\eta_y^2})], \tag{19}$$

$$\gamma=\sqrt{\frac{\overline{\eta_x^2}+\overline{\eta_y^2}-\sqrt{(\overline{\eta_x^2}-\overline{\eta_y^2})^2+4\overline{\eta_x\eta_y}}}{\overline{\eta_x^2}+\overline{\eta_y^2}+\sqrt{(\overline{\eta_x^2}-\overline{\eta_y^2})^2+4\overline{\eta_x\eta_y}}}}, \tag{20}$$

$$\theta_k=\tan^{-1}\left[\frac{\sqrt{\overline{\eta_t^2}}\sqrt{(\overline{\eta_t\eta_y})^2\cdot\overline{\eta_x^2}-2\overline{\eta_t\eta_x}\cdot\overline{\eta_t\eta_y}\cdot\overline{\eta_x\eta_y}+(\overline{\eta_t\eta_x})^2\cdot\overline{\eta_y^2}}}{(\overline{\eta_t\eta_x})^2+(\overline{\eta_t\eta_y})^2}\right], \tag{21}$$

where η_t, η_x and η_y are the heave velocity, the pich and the roll angles of the buoy respectively.

3. Facilities and Procedure of Observation

3.1 Wave Observation Buoy

The buoy employed for the wave and weather observation is a discus buoy with the diameter of 10 meters. Many bouys of this type have been operated as ocean weather stations by the Japan Meteorological Agency. The buoy (which is called the Nojima station hereafter) was placed at a location about 850 kilometers to the east-southeast of Cape Nojima (see Fig. 1), i.e., 147°E in longitude, 32°N in latitude and 6,000 m in depth, in October 1983.

The buoy was equipped with a HIPPY-120 (product of the Datawell Co., Netherlands) for heave, pitch and roll measurements in addition to weather measuring equipments. The size and some specifications of the sensor are listed in Table 1. The sensor has an AD converter and produces digital signals as well as analogue signals. System

Table 1 Specifications of pitch and roll sensor (Hippy-120)

Item	Specification
Size and weight	Cylindrical container (66 cm in diameter 84 cm in height), 120 kg
Natural period	120s (the stabilized platform)
Range of measurement	Pitch and roll ± 90 degrees (linearity error : less than 1.5%) heave acceleration ±10m/s² (do : 1.5%) analog and digital integrated heave ±10m (do : 1.5%)
Output range	±10V (analogue), 2048 bit (digital) full scale
Bandwidth	0.067−1 Hz

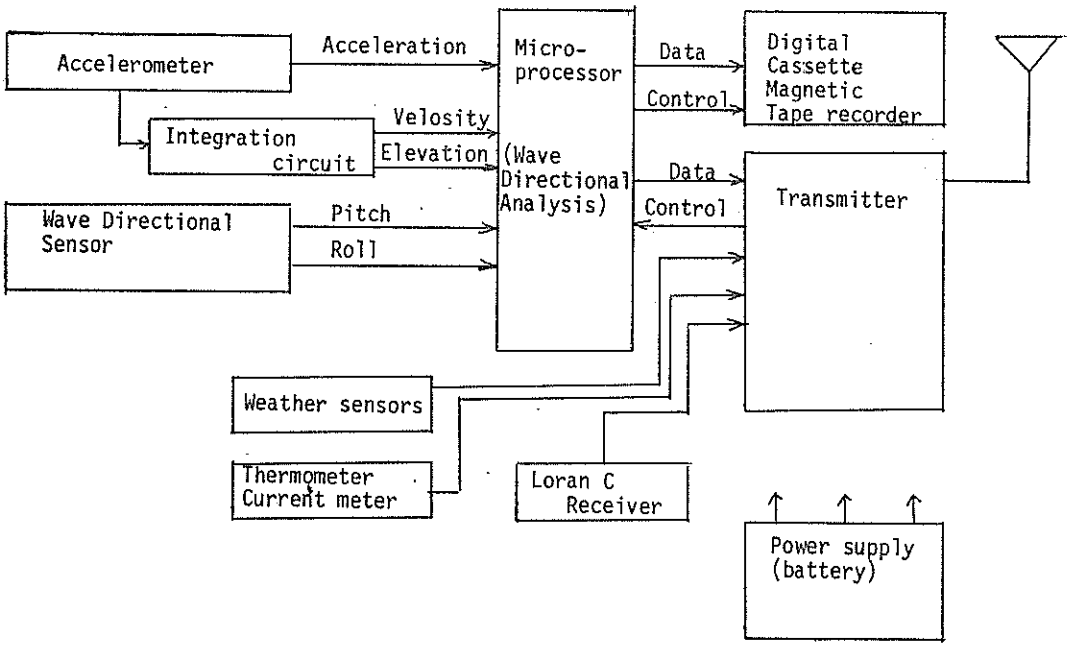

Fig. 3 System Setup in the buoy

setup in the buoy is schematically shown in Fig. 3. The buoy measured weather and waves every three hours for about 8 months until it was brought back ashore in June 1984.

During each observation, the digital output signals were analized immediately by several microprosessors on board and the results were transmitted every three hours to the Japan Meteorological Agency via the geo-stationary satellite. The raw digital signals were also recorded directly in three digital magnetic tape recorders. Unfortunately, however, all the three recorders had stopped working within the first two weeks of the observation because of tangling troubles of magnetic tapes.

3.2 Quantities Measured

The quantities, obtained through the satillite communication, are listed in Table 2 with their ranges of measurements. Among these quantities, the following items are the results of the on-board analysis by the algorithm described below.

(1) Mean wave height and period of 20 waves ($\overline{H}_{20}$, $\overline{T}_{20}$)

The water level fluctuation is calculated by integrating the heave acceleration twice with respect to time. The individual waves are defined by zero-upcrossing method. The value $\overline{H}_{20}$ and $\overline{T}_{20}$ are calculated by *Eq* (22) respectively, and they are the mean of the heights and the periods of the first 20 waves during a 20-minute long observation.

$$\left.\begin{aligned}\overline{H}_{20}&=\frac{1}{20}\sum_{i=1}^{20}H_i,\\ \overline{T}_{20}&=\frac{1}{20}\sum_{i=1}^{20}T_i.\end{aligned}\right\} \tag{22}$$

It should be mentioned here that the water level data for $\overline{H}_{20}$ and $\overline{T}_{20}$ were obtained

Table 2 Quantities transmitted from the buoy (wave observation)

Quantity	Symbol	Range	
Wind direction	θ_w	0−360°	
Wind speed	U	0−120 knot	
Mean wave height (20 waves)	$\overline{H}_{20}$	0−20m	(zero up-crossing)
Mean wave period (20 waves)	$\overline{T}_{20}$	0−20 s	(do)
Buoy orientation		0−360°	
Significant wave height	H_s	0−20m	($4.0\times\eta_{rms}$)
Mean wave height	$\overline{H}$	0−20m	
Mean wave period	$\overline{T}$	0−20 s	
Maximum wave height	H_{max}	0−20m	(zero up-crossing)
Maximum wave period	$\overline{T}$	0−20 s	(do)
Skewness	$\sqrt{\beta_1}$	±5.00	
Kurtosis	β_2	0−10.0	
Mean wave direction	$\overline{\theta}$	±90°	
Principal wave direction	θ_p	±45°	
Long-crestedness	γ	0−1.0	
Mean spreading angle	θ_k	0−90°	

by an independent heave accelerometer.

(2) Significant wave height(H_s)

The significant wave height is defined as the mean of the wave heights of the one-third highest waves among all the individual waves (H_1, ···, H_n) which appear during a 20-minute long observation. Generally, one measurement for 20-minute contains a record of about 100 to 200 individual waves. Therefore, the computation of significant wave height on the basis of this definition requires storages of 100 to 200 wave heignts and periods, and it has to be performed after the observation is over.

In order to save the capacity of on-board microprocessors and to shorten the data processing time, the significant wave height H_s was estimated from the root-mean-square value of the water level fluctuation by the following equation:

$$H_s=4.004\ \eta_{rms}, \tag{23}$$

where

$$\eta_{rms}=\sqrt{\frac{1}{n}\sum_{i=1}^{n}(\eta_i-\overline{\eta})^2}, \qquad \overline{\eta}=\frac{1}{n}\sum_{i=1}^{n}\eta_i, \tag{24}$$

and η_i denotes the water level digitized with a sampling interval one second, and $n=1,200$.

Equation (23) is derived on the basis of the assumption that the probability density of the indvidual wave heights of a wave group follows the Rayleigh distribution, Eq. (25).

$$p(x)=2a^2x\exp[-a^2x^2], \tag{25}$$

where

$$x=H_i/\eta_{rms}, \qquad a=1/2\sqrt{2}. \tag{26}$$

(3) Mean wave height ($\overline{H}$) and period ($\overline{T}$)

A mean wave height and period are calculated respectively as the mean of the heights and the periods of all the individual waves by Eq. (27).

$$\overline{H}=\frac{1}{n}\sum_{i=1}^{n}H_i, \qquad \overline{T}=\frac{1}{n}\sum_{i=1}^{n}T_i. \tag{27}$$

(4) Maximum wave height(H_{max}) and period (T_{max})

The maximum wave height and the period are the height and the period of the individual wave having the largest wave height of the whole wave group.

(5) Mean wave direction ($\bar{\theta}$) and the principal wave direction (θ_p)

The mean wave direction and the principal wave direction are calculated from the covariances of the time series of the heave speed, pitch and roll of the buoy by Eqs. (18) and (19), respectively, as stated in 2.

The on-board processing does not take into account the fluctuation of the buoy orientation. Hence, $\bar{\theta}$ and θ_p are the directions calculated in the coordinates fixed to the buoy. Therefore, the true wave directions are calculated afterwards in the process of laboratory data analyses by adding the difference between the average buoy orientation measured by a magnetic compass on board during the 20-minute observation and the magnetic north.

(6) Long-crestedness and mean spreading angle

The long-restedness and the mean spreading angle are also computed from the covariances of the three quantities related to the buoy motion by Eqs. (20) and (21), respectively.

(7) Skewness and Kurtosis

The skewness and kurtosis are the indices which show the extent of the deviation of the probability density of water level η_i from the normal distribution, and thus they indicate the magnitude of nonlinear behavior of wave motion. These two indices are defined by Eqs. (28) and (29), respectively. The kurtosis also serves as an indicator of the degree of contamination by spike noises. When the probability density of the water level η_i is well expressed by the normal distribution, the skewness takes the value zero and the kurtosis is equal to 3.0.

$$\text{Skewness} \quad \sqrt{\bar{\beta}_1}=\frac{1}{\eta_{rms}{}^3}\cdot\frac{1}{n}\sum_{i=1}^{n}(\eta_i-\bar{\eta})^3, \tag{28}$$

$$\text{Kurtosis} \quad \beta_2=\frac{1}{\eta_{rms}{}^4}\cdot\frac{1}{n}\sum_{i=1}^{n}(\eta_i-\bar{\eta})^4. \tag{29}$$

3.3 Examination of Directional Sensor

Prior to the in situ observation, the response characteristics of the directional sensor to be installed on the buoy was examined.

(1) Examination of heave response

The sensor Hippy 120 was installed on a 1/10 scale model of the discus buoy, and tested for periodic waves in a wave channel with 105 m in length, 3.0 m in width and 2.5 m in depth. The motion of the buoy was shot by a video camera. The heave amplitude was visually measured on the video screen afterwards. The amplitudes of the analogue and digital signals of the sensor are compared with those visually measured in Fig. 4. The correlation between the amplitude measured by two different ways is quite good. Also there is no substantial difference observed between the analogue and the digital signals of the sensor.

The sensor response was further tested for large amplitude motions by vibrating the sensor vertically with the use of about 10 m long rubber strips hanged from the top of a crane. The sensor was given an initial displacement by lifting or pulling down manually

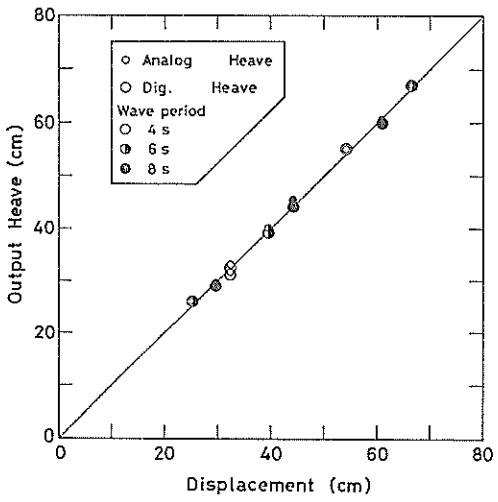

Fig. 4 Correlation between Elevation and Heave Output

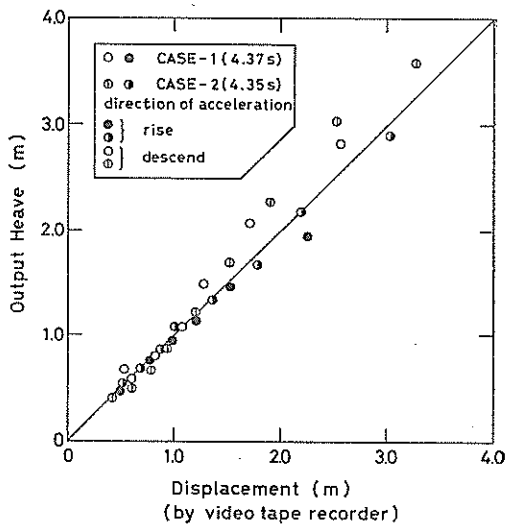

Fig. 5 Correfation between Elevation(from VTR) and Heave Output

from the equilibrium position and was released to start a free damping oscillation. While the sensor was oscillating, the positions of the upper and the lower dead points of the motion were visually measured with the aid of a video camera and a video tape recorder. The results were compared with the maxima and the minima of the output signals of the sensor as shown in Fig. 5. Although a slight scattering of the data from the line of perfect agreement is observed owing to the error brought by the visual measurements, the correlation can be said to be sufficiently good.

(2) Examination of pitch and roll response

The response of the directional sensor for pitch and roll was first examined statically. A platform was prepared to incline the sensor. The platform was a rectangular board which has a hinge on one end to be fixed on the bed. The other end of the platform was movable vertically and was lifted and lowered by a chain block. The position of the movable end was measured with a scale and the inclination of the platform was obtained through the simple geometric calculation. This static tests were performd for different sensor orientations to the direction of the platform inclination. The pitch and the roll angles of the sensor were calculated by the following equations and compared with the sensor outputs.

$$\left.\begin{aligned}\sin(\text{pitch angle}) &= \sin\alpha \sin\phi,\\ \sin(\text{roll angle}) &= \sin\alpha \cos\phi,\end{aligned}\right\} \tag{30}$$

where α is the inclination of the platform and ϕ denotes the angle between the sensor orientation and the direction of the platform inclination.

The difference between the sensor outputs and the calculated roll angles is shown in Fig. 6. The relative error is approximately less than 1.5%, which is consistent with the specification given by the manufacturer.

The pitch and roll response of the sensor was tested during the scale model tests for periodic waves. For the waves having small amplitudes, the motion of the buoy was measured by a six-component displacement meter, which is a standard equipment for ship

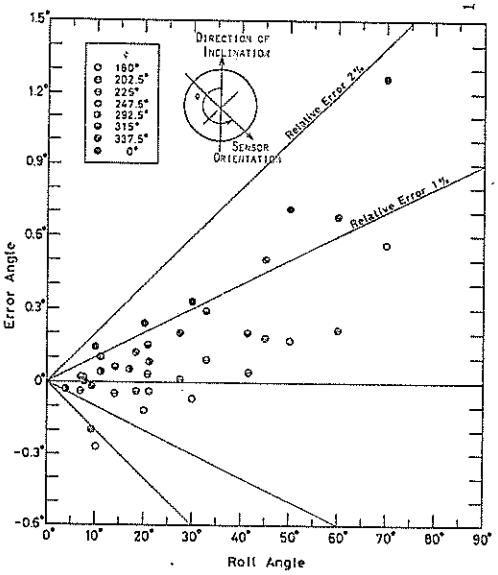

Fig. 6 Relative Error of Roll Output

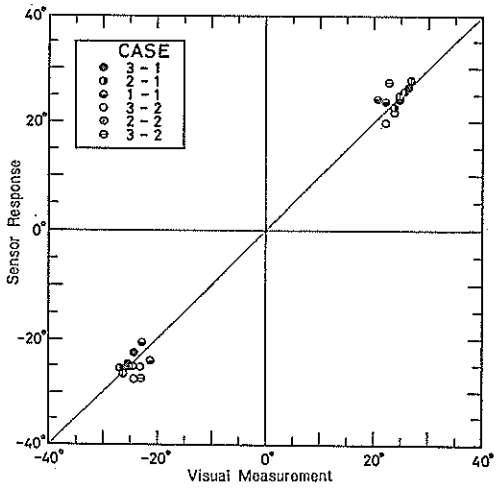

Fig. 8 Correlation between Sensor output and Inclination of Sensor

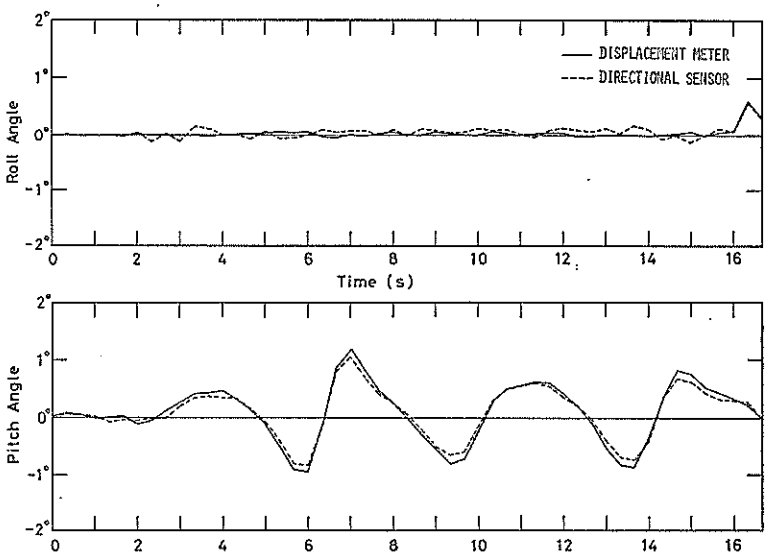

Fig. 7 Response of Pitch and Roll Output

motion tests. An example of the records of the pitch and roll sensor and the displacement meter is shown in Fig. 7. The signals from the two equipments are in good agreement.

The pitch and roll response was further tested for larger amplitude motions dynamically by the use of a large pendulum hanged from a crane. The sensor inclination at the right and the left dead points of the swing motion were measured visually utilizing a video camera and a video tape recorder (VTR). Figure 8 shows the comparison between

the sensor output and the inclination measured from VTR. The correlation between the sensor inclination measured by these two different ways can be said to be quite acceptable, if consideration is given to the possibility that some error might be entrained in reading the sensor inclination on the video screen.

4. Results of Observation

4.1 Statistical Characteristics of Wave Parameters

The analysis in this report was made for the wave data obtained over the period from October 18 of 1983 to March 31 of 1984; several storm waves recorded during this season.

The means and the standard deviations of representative wave quantities have been calculated over the period of 6 months, and the results are listed in Table 3. The mean of the skewness is very close to zero, and the mean of the kurtosis is very close to 3.0. It is said, therefore, that the water surface motion exhbited linear characteristics and the contamination of the sensor signals by spike noises was minimal.

The mean of the significant wave height is 3.35 m, while the coastal wave observation has yielded the mean significant wave height of 1.8 m at Habu Port, Oshima Island (139°27′18″E, 34°40′23″N, water depth 50 m) and the value of 1.1 m at Hitachinaka Port (140°39′36″E, 36°23′24″N, water depth 30 m). The difference implies that in the sea area of the present interest (which is called the Nojima sea area hereafter) large waves with the heights twice to three times those observed in the coastal area are seen almost continuously. It should be noted that the significant wave height exceeded 4 m for about a half of the period from January through February in 1984. The average of the mean wave period during the whole observation was 7.3 s, which is about one second longer than those observed at the two coastal stations. These defferences between the wave heights and periods obtained at the Nojima station and the two coastal stations might have resulted from the difference in the fetch length for the predominant northwestern monsoon which generated the waves in the Northwestern Pacific Ocean.

As to the relation between some characteristic wave parameters, the mean of the ratio H_{max}/H_s (1.46) is slightly smaller than that at coastal area (1.55 to 1.77)[8], while

Table 3 Wave Statistics

Quantity	Mean (standard deviation)	Quantity	Mean (standard deviation)
H_s	3.35m(1.25m)	H_{max}/H_s	1.46(0.16)
H_{max}	4.88m(1.91m)	$H_s/\overline{H}$	1.72(0.09)
$\overline{H}$	1.97m(0.77m)	$\overline{H}/\overline{H}_{20}$	0.93(0.07)
$\overline{H}_{20}$	2.12m(0.81m)	$H_{max}/\overline{H}$	2.50(0.30)
T_{max}	9.00 s (1.68 s)	$T_{max}/\overline{T}$	1.23(0.17)
$\overline{T}$	7.31 s (1.04 s)	$\overline{T}/\overline{T}_{20}$	0.86(0.10)
$\overline{T}_{20}$	8.56 s (1.16 s)	$T_{max}/\overline{T}$	1.06(0.17)
$\sqrt{\beta_1}$	0.044 (0.064)	θ_k	56.2°
β_2	3.005 (0.230)	γ	0.82

Regression equation	Correlation coefficient
$H_{max}=1.458\ H_s-0.03$	0.954
$H_s\ =1.614\ \overline{H}-0.176$	0.992
$\overline{H}\ =0.934\ \overline{H}_{20}-0.008$	0.977
$H_{max}=2.357\ \overline{H}+0.374$	0.948
$H_{max}=2.213\ \overline{H}_{20}+0.201$	0.932

the ratio $H_s/\overline{H}$ (1.72) is slightly larger than that at the coastal stations (1.50 to 1.61). These differences are supposed to have resulted from the overestimation of the significant wave height, because the significant wave height at the Nojima station was calculated by the relation $H_s=4\eta_{rms}$. It is a well established fact that the wave-by-wave analysis of the coastal wave data yields the approximate relation $H_s=3.8\eta_{rms}$ on the average. If the latter relation is applied to estimate the significant wave height at the Nojima station, the value of H_s in Table 3 decreases by 5 percents to 3.18 m. Hence the ratios H_{max}/H_s and $H_s/\overline{H}$ become in 1.53 and 1.63, respectively. These values are almost the same ratios obtained from coastal wave records.

It should also be noted that the correlation between the full mean wave height $\overline{H}$ and the mean height of the first 20 waves $\overline{H}_{20}$ is quite good, for the correlation coefficient is 0.977. In addition the mean of the ratio $\overline{H}/\overline{H}_{20}$ is 0.93 and the standard deviation of it is less than 8%. Thus, it can be said that even a short wave record may yield a good estimate of the wave parameters related to wave height statistics, even though its statistical reliability is not high.

The mean of the ratio $\overline{T}/\overline{T}_{20}$ is 0.86. This indicates that the mean wave perids for 20 waves are longer than those for whole records. This difference may have resulted from the different response characteristics between the accelerometers employed in the measurements of $\overline{H}_{20}$ and $\overline{T}_{20}$ and the accelerometer of Hippy-120.

The cumulative distribution of the significant wave height at the Nojima station is compared with those at the two coastal stations in Fig. 9. The Distributions have been normarized with the mean values of the significant wave height at respective stations. The distribution curve shown with the open circles is the one for the Nojima station, and it shows the tendency very similar to that for Habu Port, while the curve for Hitachinaka Port shows a little different tendency.

The joint distribution of wave height and period at the Nojima sea area over the three-month period of December through February is shown in Fig. 10. The figures in Fig. 10 are the number of observations which fall on respective ranges of the height and period. The abscissa denotes the significant wave period which has been converted from the mean wave period by using the relation $T_s=1.1\overline{T}$ obtained at coatal stations, while

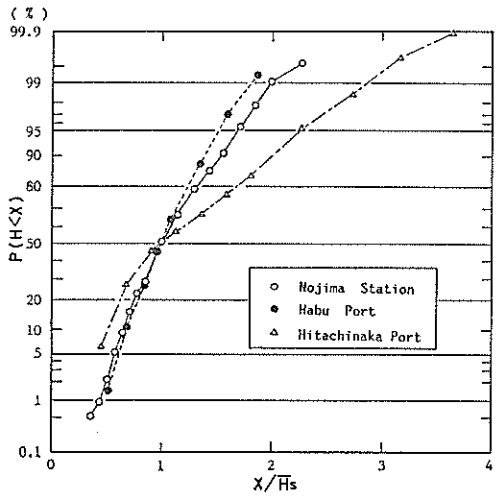

Fig. 9 Cumulative Distribution of Significant Wave Height

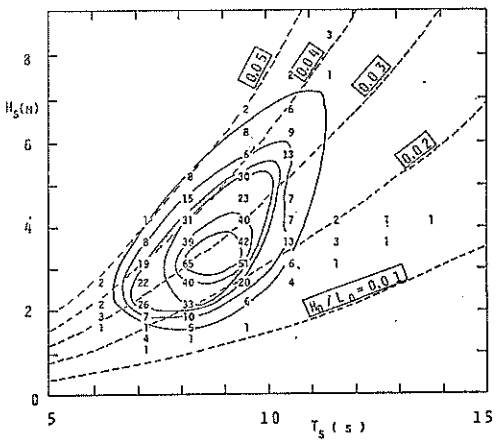

Fig. 10 Joint Distribution of Wave Heights and Periods (Nojima Station)

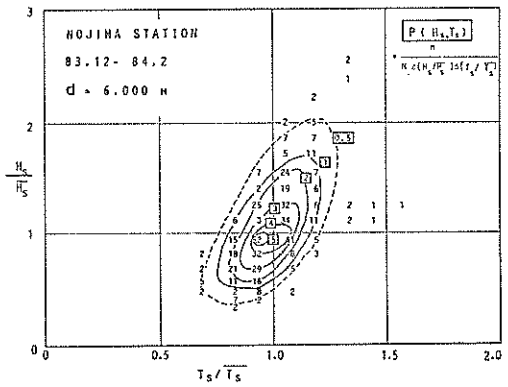

Fig. 11 Joint Distribution of Nondimensioned Significant Wave Heights and Periods (Nojima Station)

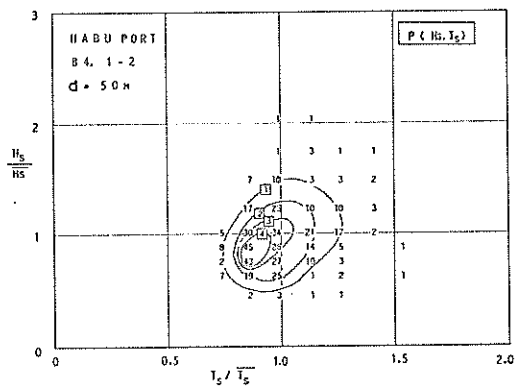

Fig. 12 Joint Distribution of Nondimensioned Significant Wave Heignts and Periods (Habu Port)

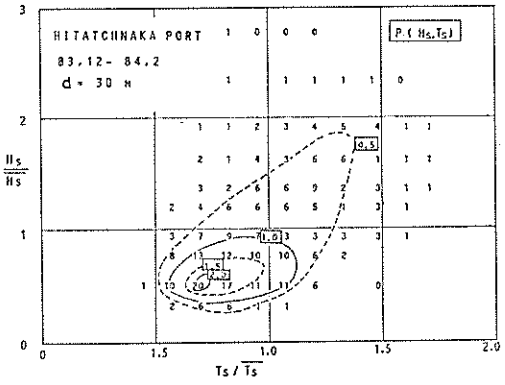

Fig. 13 Joint Distribution of Nondimensioned Significant Wave Heights and Periods (Hitachinaka Port)

the ordinate denotes the observed significant wave heights. Figure. 10 shows that most of the waves occurring in the Nojima sea area have the wave steepness (H_0/L_0) ranging from 0.02 to 0.04, which is the characteristics of waves under wind action. Among the wave group with the significant wave height exceeding 5 m, the steepness seems to approach the value 0.04. The same tendency has been observed in the coastal wave data[9].

The joint distribution of the significant wave height and period relative to the overall mean values during the three-month period is shown in Fig. 11 for the Nojima station and in Figs. 12 and 13 for the two coastal stations. The figures in Figs. 11 to 13 are the values of the probability density for respective values of $H_s/\overline{H}_s$ and $T/\overline{T}_s$. The probability density is calculated by

$$P(H_s/\overline{H}_s,\ T_s/\overline{T}_s)=n/N[\Delta(H_s/\overline{H}_s)\Delta(T_s/\overline{T}_s)], \tag{31}$$

where n denotes the number of observations which fall on respective range and N denotes total number of observation druing the three months. The values of the probability density are multiplied by 10 and shown with one or two digits in Figs. 11 to 13. The figures surrounded by squares indicate the absolute values of the probability density for respective contour lines.

A noticeable difference between the joint distributions of the Nojima station and the two coastal stations is the degree of the correlation between the wave height and period. The correlation is high at the Nojima station while it is low at the coastal stations. The difference suggests that the energy of swell from remote areas is not conspicuous in the Nojima sea area compared with that at the coastal area. It can be said therefore that the big waves in the Nojima sea area mainly consist of wind waves generated in the sea area nearby.

4. 2 Characteristics of Extreme Seas

Typical records of the wave and weather data of extreme seas are shown in Figs. 14

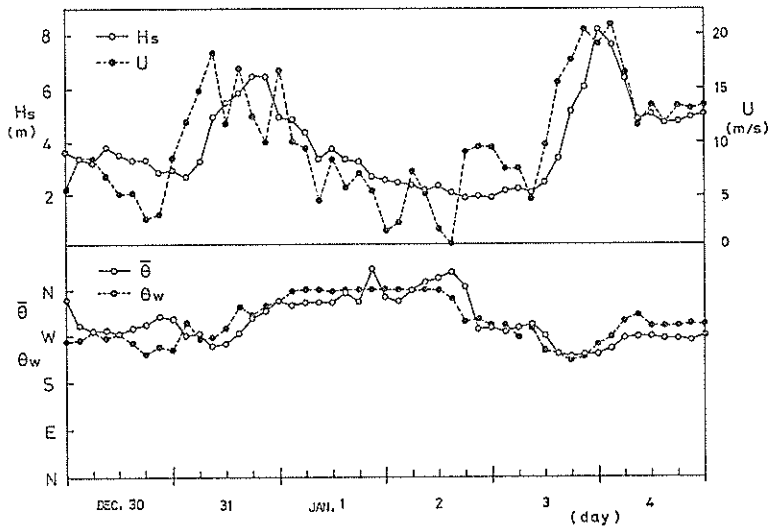

Fig. 14 Time Variation of Waves and Winds at Nojima Station (Dec. 30, 1983–Jan. 4, 1984)

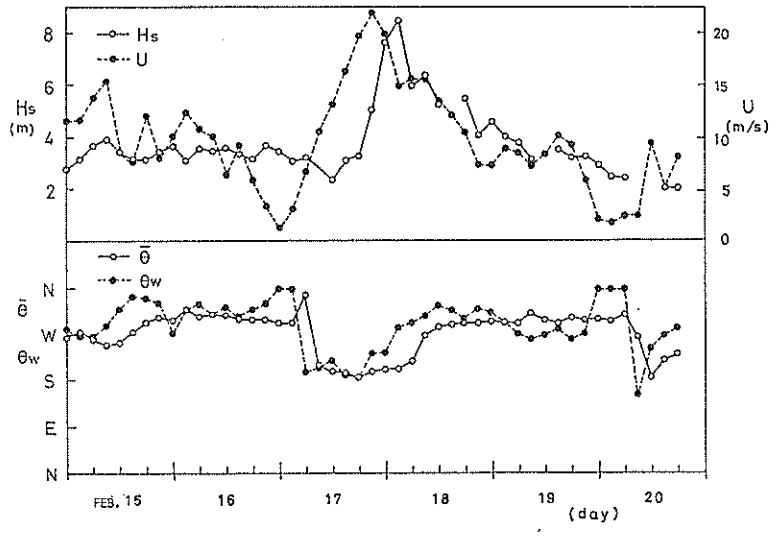

Fig. 15 Time Variation of Waves and Winds at Nojima Station (Feb. 15–Feb. 20, 1984)

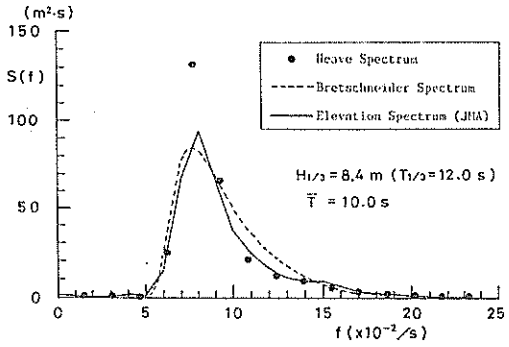

Fig. 16 Wave Spectrum (at 0300, Feb. 18)

and 15. In these figures the time variation of significant wave height and that of wind speed are compared with each other in the upper half, and the comparison between the time variations of the mean wave direction and the wind direction is shown in the lower half. It is seen that the variations of the significant wave height and the mean wave direction closely follow the changes of the wind speed and direction respectively, with some delay. Generally speaking, extreme sea states appear when the wind speed increases beyond 15 m/s immediately after a sudden change of the wind direction from the northwest to the southwest. As the wind speed increases, the wave height increases within the time span of 12 to 15 hours.

Figure 16 shows the power spectrum of the waves observed at 0300 on February 18, when the significant wave height recorded the largest value 8.33 m. The closed circles show the heave spectrum obtained from the directional sensor. The solid line denotes the spectrum estimated from the reproduced wave profile on the basis of the transmitted data of the crest and trough heights as well as the time intervals between them, by using the technique of interpolation. The reproduction of the wave profile and the spectral analysis were made by the Japan Meteorological Agency. The spectral peak appears at the frequency of 0.08 Hz (corresponding to the period 12 s), and most of the wave energy is concentrated within a frequency range between 0.06 to 0.15 Hz. The broken line in Fig. 16 is the Bretschneider-Mitsuyasu type frequency spectrum which is given by Eq. (32).

$$S(f)=0.257H_s^2T_s(T_sf)^{-5}\exp[-1.03(T_sf)^{-4}] \tag{32}$$

In the calculation of the frequency spectrum by Eq. (32), the observed significant wave height H_s=8.33 m is employed and the significant wave period T_s is given as 12.0 s which is the reciprocal of the peak frequency of the observed spectrum. The observed spectrum has a sharper peak than the Bretschneider-Mitsuyasu spectrum, which suggests strong wind action over a relatively short fetch.

The maximum significant wave heights observed during some extreme sea states as well as the date and the time of the occurrence are compared with those observed at the coastal stations as shown in Table 4. It is seen that the extreme sea states at the Nojima sea area and the coastal area occurred almost simultaneously.

As discussed in the above, the variations of the wave height and the wave direction

Table 4 Comparison of Extremes

Date	Nojima Station			Habu Port			Hitachinaka Port		
	Time	H_s	$\overline{H}(\overline{T})$	Time	$H_s(T_s)$	$\overline{H}(\overline{T})$	Time	$H_s(T_s)$	$\overline{H}(\overline{T})$
Jan. 26	1200	7.92m	5.02m (9.0 s)	1200	2.92m (7.9 s)	1.88m (7.2 s)	0600	2.36m (12.2 s)	1.42m (8.4 s)
Feb. 18	0300	8.44m	5.02m (10.0 s)	1200	3.13m (9.1 s)	1.91m (7.3 s)	0600	3.08m (6.7 s)	2.00m (5.8 s)
Feb. 27	1800	8.04m	4.80m (10.0 s)	0000	3.89m (8.0 s)	2.51m (7.6 s)	0400	2.50m (9.3 s)	1.56m (7.5 s)

are closely correlated with the changes of the wind speed and direction. It is also found that the power spectrum of the extreme sea state is similar with the Bretschneider-Mitsuyasu type spectrum which represents a standard shape of the spectrum of fully developed wind generated waves in deep sea. Therefore, for extreme seas, it can be said that the waves in the Nojima sea area are mainly contributed by the wind waves generated over this sea area and the contribution of swell from remote sources is not large.

5. Estimation of Directional Wave Spectrum

5.1 Characteristics of Directional Parameters at Nojima Station

In this chapter the characteristics of directional wave spectrum is examined from the viewpoint of the two directional parameters, i.e., the long-crestedness and the mean spreading angle, because of the lack of full records of heave, pitch and roll data.

When the directional spectrum is characterized by the Bretschneider-Mitsuyasu frequency spectrum (Eq. 32) coupled with the Mitsuyasu type directional function (Eq. 7), the two directional parameters can be calculated as the function of the spreading parameter s_{max}. The calculation with various values of s_{max} has shown that there exists a consistent relation between the long-crestedness and the mean spreading angle, as shown by the solid line with the closed circles in Fig. 17.

Calculation has further been carried out for the cases of bimodal directional

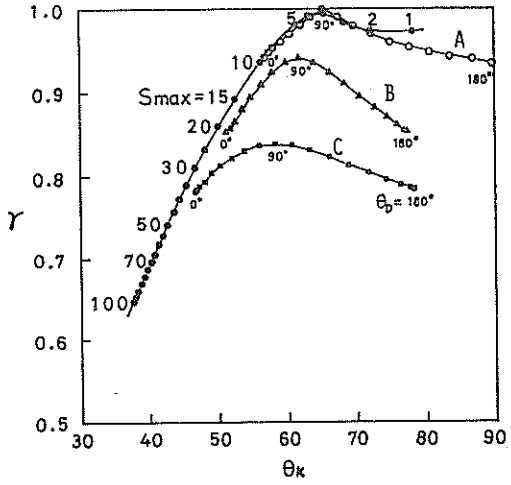

Fig. 17 Relation between Long-crestedness γ and Mean Speading Angle θ_k

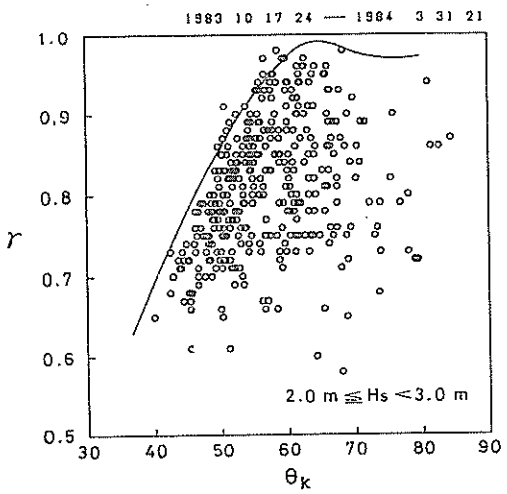

Fig. 18 Observed Values of γ and θ_k (1)

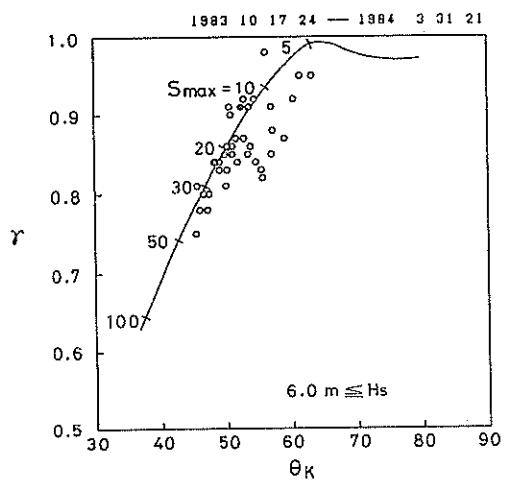

Fig. 19 Observed Values of γ and θ_k (2)

wave spectra, which are given as the superposition of the two unimodal wave spectra specified by the Bretschneider-Mitsuyasu power spectrum and the Mitsuyasu type directional function. The difference between the two mean wave directions, which is designated by θ_D, are varied from 0° to 180°. In addition to the result of the calculation for unimodal spectra, Fig. 17 above shows the results for the cases of bimodal spectra. The line denoted with the symbol A represents the case in which two wave groups of identical characteristics with $s_{max}=10$ interact. The line B is drawn for the case in which one wave group is the wind waves with $s_{max}=10$ and the other is the swell with the wave height being one half of the former, with $s_{max}=100$ and with the same wave period as the former. The line C shows the case in which the wind waves and the swell have the same energy and significant period, but the spreading parameter is $s_{max}=10$ for the former and 100 for the latter.

The three lines A, B and C for the bimodal spectra appear in the right-hand side of the line for the unimodal spectra, and the deviations of these lines from the latter are quite large, especially when θ_D is larger than 90°. This tendency of the lines for the bimodal spectra results from such characteristics of the long-crestedness that it takes the maximum value for $\theta_D=90°$ and decreases as θ_D increases beyond 90°. Because of this characteristics, the long-crestedness itself cannot be an appropriate index of directional spreading. However, coupled with the other parameter, i.e., the mean spreading angle θ_k, it can serve as a very useful auxiliary parameter to distinguish bimodal seas from unimodal ones.

The data of the long-crestedness and the mean spreading angle of the Nojima station are compared with the theoretical relation for unimodal spectra in Figs. 18 and 19. Figure 18 shows the comparison for the group of waves having smaller significatnt wave heights ($H_s=2$ to 3 m), while Fig. 19 shows the data of the group of waves with larger heights. In both figures, the solid line representing the relation for waves with unimodal spectra provides an envelope of the observed data which are scattered in the right-hand side of the line. As for the group of waves with smaller wave heights, the range of scatter is very wide. This suggests that the directional spectra of smaller waves have very complicated shapes, probably with coexistence of several groups of waves from various generating sources. On the other hand, in the case of extreme seas with the significant wave heights larger than 6 m (Fig. 19), the range of scatter is small and the solid line well approximates the observed data of the two directional parameters.

From the comparison of the extent of the scatter of γ and θ_k data for extreme seas in Fig. 19 with the theoretical curves in Fig. 17, it can be deducted that extreme seas in the Nojima sea area have a unimodal wave spectrum with s_{max} ranging from 10 to 40. If it is assumed that they are waves with bimodal directional spectra, the difference in their mean directions should be less than 90°.

Incidentally, the mark of filled circle in Fig. 19 represents the data of the largest significant wave height observed at 0300 on Feb. 18, and the values of γ and θ_k corresponds to the case of unimodal spectrum with $s_{max}=12$ or 13.

5.2 Characteristics of Directional Parameters at Coastal Stations

As discussed in 5.1, whether a directional wave spectrum is unimodal or bimodal can be judged from the values of γ and θ_k. These directional parameters have been calculated from the wave data obtained at Hitachinaka Port and Niigata Port (139°05′19″E, 37°58′47″N, water depth 22.7 m, Japan Sea coast), where the directional wave measurements are made utilizing two-axis current meters. Figure 20 shows the theoretical relation between γ and θ_k drawn for the directional measurement with the current meters in the same manner as Fig. 14. Since the values of the parameters are calculated from the covariances between the water surface elevation and the horizontal velocity

components calculated at the level of 2 m above the sea bed, the lines in Fig. 20 is slightly different from those shown in Fig. 14, because of the nature of the transfer functions from the water surface elevation to velocity components. The data of γ and θ_k calculated from the records obtained at Hitachinaka Port are compared with the theoretical curves in Figs. 21 and 22. When the significant wave height exceeds 2.0 m (Fig. 21), the re-

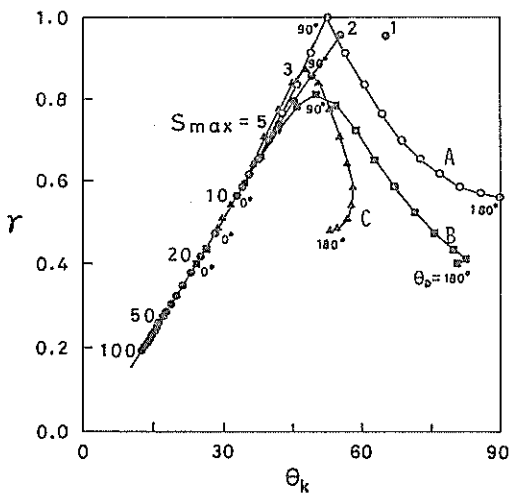

Fig. 20 Relation between γ and θ_k (Hitachinaka Port)

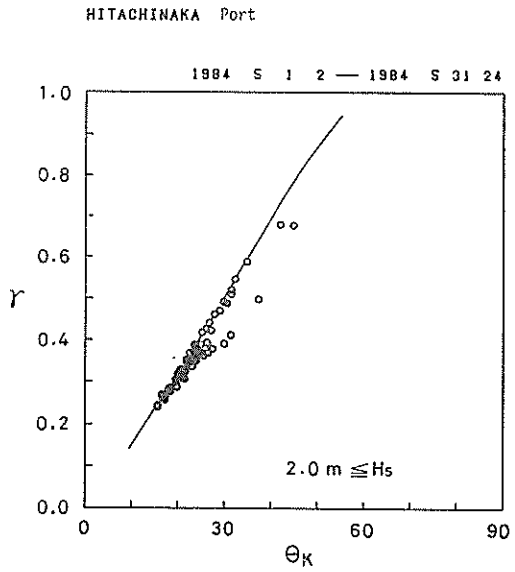

Fig. 21 Observaed Values of γ and θ_k (1)

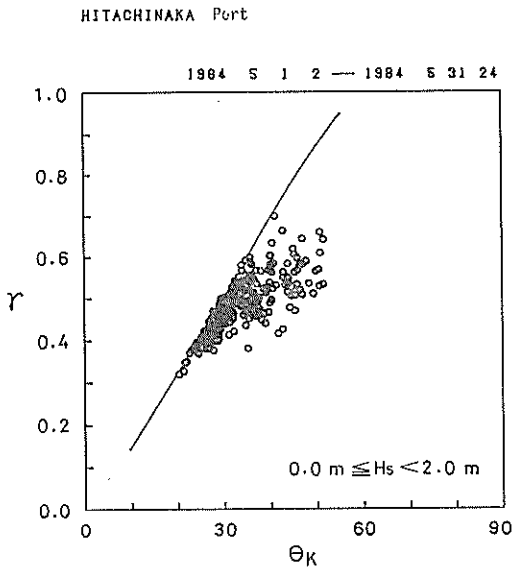

Fig. 22 Observed Values of γ and θ_k (2)

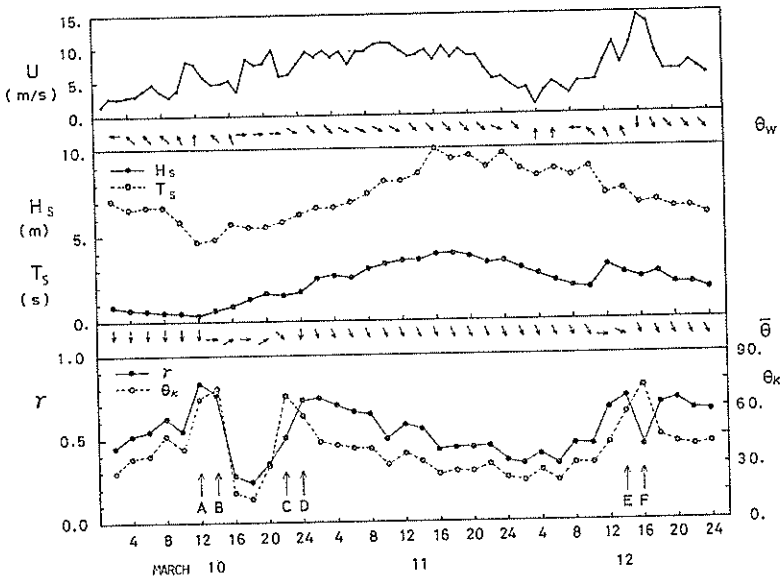

Fig. 23 Time Variation of Wind, Wave and Parameters at Niigata Port (March 10-12, 1984)

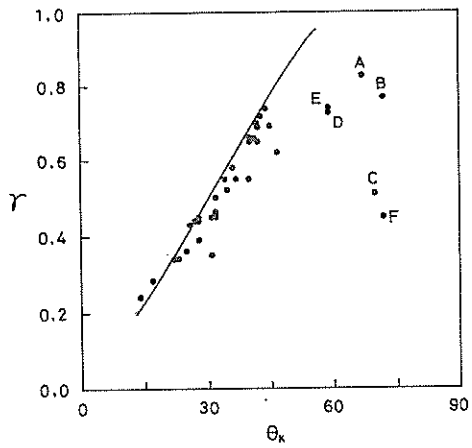

Fig. 24 Observed Values of γ and θ_k (Niigata Port)

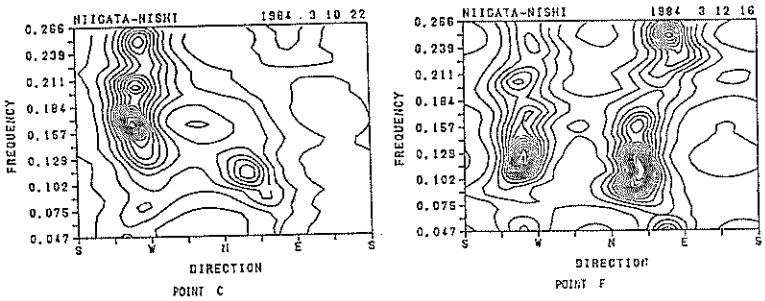

Fig. 25 Estimated Directional Wave Spectrum

lations between the observed values of γ and θ_k are well approximated by the theoretical curve drawn for unimodal directional spectra, while the data of γ and θ_k for the group of waves with smaller significant wave heignts appear in a scattered manner in the right hand side of the curve (Fig. 22).

Wave data obtained at Niigata Port are also analyzed in the same way. Figure 23 shows the time variations of wind speed (U), wind direction (θ_w), significant wave height (H_s) and period (T_s), mean wave direction ($\bar{\theta}$), the long-crestedness (γ) and the mean spreading angle (θ_k), for the 3-day period of relatively rough seas from March 10 to March 12, 1984. The values of γ and θ_k are compared with the theoretical relation for the unimodal spectra in Fig. 24. During the three days, the observed values of γ and θ_k fall on the vicinity of the theoretical curve for unimodal spectra, except six observations denoted with A to F. As seen in Fig. 23, all these exceptional points A to F, which exhibit large deviations from the theoretical curve in Fig. 24, take place immediately after the wind direction had changed. Such changes in the wave direction should have been associated with the presence of bimodal spectra. As an example, the directional spectra at 2200 on March 10 (Point C) and at 1600 on March 12 (Point F) have been calculated by the extended maximum likelihood method and is illustrated in Fig. 25. Clearly, two directional peaks are observed, which proves the presence of bimodal spectrum. Thus, the characteristics of directional spectra are well recognized by using the relation between the long-crestedness and the mean spreading angle.

6. Conclusions

Summing up the results of the study described above, the following is the major conclusions.

1. The waves occurring in the Nojima sea area during the winter are twice to three times larger than those observed in the coastal sea area. However, the ratios between characteristic wave parameters, such as H_{max}/H_s and $H_s/\overline{H}$, are similar to those observed in coastal sea area.
2. The correlation between the relative significant wave height ($H_s/\overline{H}_s$) and the relative period ($T_s/\overline{T}_s$) at the Nojima station is higher than that observed in coastal sea area, and the steepness of most of the waves occurring in the Nojima sea area is ranging from 0.02 to 0.04, which is the characteristics of the waves under wind action.
3. The significant wave height and the mean wave direction clearly follow the change of the wind speed and the wind direction at the station, respectively. For extreme sea states, the wave power spectrum is similar to the standard shape of the spectrum of fully developed wind waves. Therefore, the contribution of swell to the extreme sea states in the Nojima sea area is much smaller than that of the wind waves generated in the sea area nearby.
4. The theoretical calculation for unimodal directional spectra yields a consistent relationship between the two parameters : the long-crestedness and the mean spreading angle. The characteristics of directional wave spectra of real sea can be well recognized by comparing the values of the two parameters with the theoretical relation. Whether a directional wave spectrum is unimodal or bimodal can be judged by the degree of the deviation of the measured values of the parameters from the theoretical relation drawn for the unimodal spectra.
5. The directional wave spectra of the extreme seas in the Nojima sea area are supposed to be unimodal one which is characterized by the Mitsuyasu type directional function

with s_{max}=10 to 40 or bimodal one which is characterized by the angular difference between the two directional peaks less than 90°.

(Received June 29, 1985)

Acknowledgement

The study presented herein was started in 1982. For the first two years, the system design of the directional wave measurement utilizing a discus buoy and the examination of the directional sensor had been conducted under the directions of Messrs. T. Takahashi and S. Murata, the formar Chiefs of the Coastal Observation Laboratory of the Port and Harbour Research Institute. Their contributions are greatly acknowledged. The authors sincerely wish to express their appreciation to Dr. Y. Goda, Deputy Director General of the Port and Harbour Research Institute, for his helpful advice on various matters ranging from the system design of the on-board analysis and the laboratory analysis of wave data. The authors also wish to express heartfelt thanks to those who were involved in the wave observation in the Japan Meteorological Agency and in the First and the Second Port Construction Bureaus for furnishing the wave data promptly, and to Messrs. Y. Kameyama and A. Narita, members of the Coastal Observation Laboratory, for their assistance in the data processing.

References

1) Longuet-Higgins, M. S., D. E. Cartwright, and N. D. Smith: Observations of directional spectrum of sea waves using the motion of a floating buoy, *Ocean Wave Spectra*, Prectice-Hall, Inc., 1963, pp. 111-136.
2) Mitsuyasu, H. et. al.: Observation of the directional spectrum of ocean sea waves using a cloverleaf buoy, *Jour. Physical Oceanography.*, Vol. 5, No. 4, 1975, pp. 750-760.
3) Capon, J., R. J. Greenfield and R. J. Kolker: Multidimensional Maximum-likelihood processing of a large aparture seismic array, *Proc. IEEE*, Vol. 55, 1967, pp. 192-211.
4) Isobe M., K. Kondo and K. Horikawa: Extension of MLM for estimating directional wave spectrum, *Simposium on description and Modeling of Directional Seas*, Danish Hydraulic Institute & Danish Maritime Institute, 1984, pp. A-6-1 - A-6-15.
5) Longuet-Higgins, M. S.: The statistical analysis of random moving surface, *Phil. Trans. Roy. Soc. London*, Ser. A(966), Vol. 249, 1956, pp. 321-387.
6) Goda Y.: Numerical examination of the measuring technique of wave direction with the 'covariance method,' *Report of P. H. R. I.*, Vol. 20, No. 3, 1981, pp. 53-92 (*in Japanese*).
7) Goda Y., K. Miura and K. Kato: On-board analysis of mean wave direction with discus buoy, *International Conference on Wave and Wind Directionality*, Édition Technip Co., 1981, pp. 339-359.
8) Takahashi, T. et. al.: Wave statistics with 10-year data in the coastal wave observation network, *Technical Note of P. H. R. I.* No. 401, 1981, 711 p. (*in Japanese*).
9) Hirose, M., Y. Tachibana and K. Sugahara: One-dimensional spectra of wind waves in coastal waters, *Report of the PHRI*, Vol 22., No. 3, 1983, pp. 83-124 (*in Japanese*).

List of Symbols

a : proportionality constant ($=1/2\sqrt{2}$)

a_n : amplitude of n-th component wave
A_n : fourier coefficients
B_n : fourier coefficients
C_{ij} : cospectra between i and j quantities
$E(l, m)$: directional wave spectrum defined in Cartesian coordinate(l, m)
f : frequency
f_n : frequency of n-th component wave
f_p : peak frequency of power spectrum
H_i : i-th individual wave defined by zero up-crossing method
$\overline{H}$: mean wave height
$\overline{H_{20}}$: mean wave height for the first 20 individual waves in a wave record
H_s : significant wave height
$\overline{H_s}$: average of the significant wave height
$H_n(\boldsymbol{k}, \omega)$: transfer function from water suface elevation to n-th wave property.
$H^*(\boldsymbol{k}, \omega)$: the complex conjugate of the transfer function $H_m(k, \omega)$
$H_{\max}$: maximum wave height
H_o : significant wave height in deep water
i : $=\sqrt{-1}$
k : wave number $(=2\pi/L)$
k_n : wave number of n-th component wave
$\bar{k}$: mean of wave numbers of the component waves
$\boldsymbol{k}$: wave number vector
L_o : wave length in deep water
l : $=k\cos\theta$
$\bar{l}$: mean of l
m : $=k\sin\theta$
$\overline{m}$: mean of m
n : number of discrete water elevation record or number of observation of which significant wave height and period falls on intervals $\Delta(H_s/\overline{H_s})$ and $\Delta(T_s/\overline{T_s})$
$\overline{PQ}$: deviation of wave number from the mean wave direction (see. Fig. 2)
Q_{ij} : quadrature spectrum between i and j quantities
R : root-mean-square of the wave number deviation from the mean wave direction
s : power of cosine function in the Mitsuyasu type directional function
$s_{\max}$: maximum value of s
$S(f, \theta)$: directional wave spectrum
$\hat{S}(f, \theta)$: estimate of $S(f, \theta)$
T : mean wave period
$\overline{T_{20}}$: mean wave period for the first 20 individual waves in a record
T_s : significant wave height
$\overline{T_s}$: average of the significant wave periods
U : wind speed
$\boldsymbol{x}_n$: location vector for n-th wave quantity
α : inclination of the directional sensor in the static test
$\sqrt{\beta_1}$: skewness
β_2 : kurtosis
$\Gamma(\ )$: Gamma function
γ : long-crestedness
ε_n : phase angle of n-th component wave
η : water surface elevation
$\overline{\eta}$: mean water surface elevation

η_i : i-th discrete data of the water surface measurement
η_{rms} : root-mean square of water surface elevation
η_t : speed of vertical motion of water surface
η_x : pitch angle
η_y : roll angle
θ : directional angle
$\bar{\theta}$: mean wave directson
θ_D : directional difference between the two directional peak of bimodal wave spectrum
θ_k : mean spreading angle
θ_n : direction of n-th component wave
θ_p : principal wave direction
θ_w : wind direction
κ : proportionality constant in EMLM
τ : delay in the calculation of covariances
ϕ : sensor orientation measured from tne direction of the slope in the static test of the directional sensor
Φ_{ij} : cross-spectrum between i and j quantities
ω_n : angular frequency of n-th component wave ($=2\pi f$)
Ψ_{ij} : covariance function